Organic & Biomolecular Chemistry

PAPER

View Article Online
View Journal | View Issue

Cite this: *Org. Biomol. Chem.*, 2014, **12**, 5382

The structure of 3-(diethylborylethynyl)pyridine: a nonplanarly arranged cyclic trimer†

Shigeharu Wakabayashi,*[a] Mitsumi Kuse,[a] Aimi Kida,[a] Seiji Komeda,[b] Kazuyuki Tatsumi[c] and Yoshikazu Sugihara[d]

Received 25th April 2014,
Accepted 22nd May 2014

DOI: 10.1039/c4ob00849a

www.rsc.org/obc

3-(Diethylborylethynyl)pyridines **2** assemble into a cyclic trimer stabilized *via* intermolecular boron–nitrogen coordination bonds both in solution and in the crystalline state. The outstanding structural features of the methoxy derivative **2b** in the crystalline state are that (1) two pyridine rings (*P*1 and *P*2) of the cyclic trimer of **2b** are almost coplanar, and the third pyridine ring (*P*3) is largely bent away from *P*1 and *P*2, and (2) *P*3 of the cyclic trimer stacks in a face-to-face fashion with one of the pyridine rings (*P*3′) of an adjacent cyclic trimer. The crystallographic study revealed that the conformation of the cyclic trimer is flexible enough to be affected by the crystal packing.

Introduction

Organoboranes have drawn much attention not only as versatile reagents in synthetic organic chemistry,[1] but also as building blocks of self-assembled macrocycles in supramolecular chemistry.[2] Our recent studies on borylpyridines that contain a boron atom as a coordination center and a pyridine ring as a ligand revealed that these compounds form the cyclic oligomeric assembly *via* intermolecular boron–nitrogen coordination bonds.[2d,e,g,h,k] However, the development of more sophisticated systems would help further for our understanding on the mechanism behind the changes in self-assembly and stability caused by structural modifications.[3]

Compound **2** containing an acetylenic linkage would be quite attractive because it allows extension of the cavity within the cyclic oligomer of borylpyridine.[4] Herein we describe the synthesis of **2** and its structure both in solution and in the crystalline state. Scrambling experiments on components **2a** and **2b** to estimate their stability in solution were performed and the relative stability, compared with 3-(diethylboryl)pyridines **1**, could be rationalized by the molecular structures and DFT calculations at the B3LYP/6-31G* level.

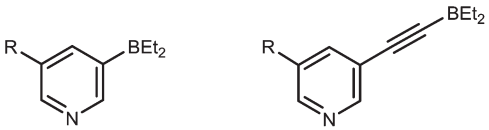

1a: R = H
1b: R = OMe

2a: R = H
2b: R = OMe

Results and discussion

Synthesis

Compounds **2a** and **2b** were prepared from the corresponding 3-ethynylpyridine.[5] Thus, the reaction of 3-ethynylpyridine with *n*-butyllithium, and then with diethylmethoxyborane in ether at −78 °C provided **2a** as colorless crystals in 72% yield. Similarly, the methoxy derivative **2b** was synthesized from 3-ethynyl-5-methoxypyridine[6] in 79% yield as colorless crystals. The expected structures were fully supported by spectral data and elemental analysis, and the compounds were stable and showed no sign of degradation after storage for one year at −20 °C.

Vapor pressure osmometry, mass spectrometry, and NMR spectroscopy

Vapor pressure osmometry (VPO) was performed using a Knauer digital vapor pressure osmometer (with benzil as the standard) to estimate the average aggregate size of the compounds. Various concentrations of **2a** in chloroform (from 0.012 to 0.083 mol dm^{-3}) at 45 °C, in benzene (from 0.011 to

[a]*Department of Clinical Nutrition, Faculty of Health Science, Suzuka University of Medical Science, Suzuka, Mie 510-0293, Japan. E-mail: s-waka@suzuka-u.ac.jp; Fax: +81-59-383-9666*
[b]*Department of Pharmaceutical Sciences, Faculty of Pharmaceutical Sciences, Suzuka University of Medical Science, Suzuka, Mie 513-8670, Japan*
[c]*Department of Chemistry, Graduate School of Science and Research Center for Materials Science, Nagoya University, Furo-cho, Chikusa-ku, Nagoya 464-8602, Japan*
[d]*Department of Chemistry, Faculty of Science, Yamaguchi University, Yamaguchi City 753-8512, Japan*

†Electronic supplementary information (ESI) available: General methods, ^{1}H and ^{13}C NMR spectra of compounds **2a** and **2b**, and ESIMS, NOESY, and ^{11}B NMR spectra of **2b**. CCDC 999215. For ESI and crystallographic data in CIF or other electronic format see DOI: 10.1039/c4ob00849a

0.077 mol dm^{-3}) at 60 °C, and in acetone (from 0.012 to 0.083 mol dm^{-3}) at 40 °C provided values of 2.8, 2.8, and 3.1, respectively. Furthermore, various concentrations of **2b** in chloroform (from 0.019 to 0.087 mol dm^{-3}) at 45 °C, in benzene (from 0.019 to 0.088 mol dm^{-3}) at 60 °C, and in THF (from 0.019 to 0.087 mol dm^{-3}) at 45 °C provided values of 3.3, 3.2, and 2.9, respectively. In each experiment, the VPO plots showed a linear relation between the concentration and the electrical differential (r = 0.995–0.999) within experimental error. These values and the clear linear relationship suggest that both **2a** and **2b** form a trimer on average in these solvents. Taking into consideration the results of ESI-MS described below, VPO data strongly suggest the presence of aggregates of $(\mathbf{2a})_3$ or $(\mathbf{2b})_3$. In contrast, the VPO plots of **2b** in DMF (from 0.017 to 0.088 mol dm^{-3}) at 90 °C were nonlinear and the modal aggregation value was nonintegral, suggesting the lack of a discrete aggregate.

In the EIMS (20 eV) spectra of **2a** and **2b**, the parent peaks (M^+) as monomer species were observed at m/z 171 (intensity 61%) and 201 (93%), respectively, as the highest mass ion peaks. These results indicate that the energy required for ionization was so high that the aggregated molecule dissociated. In contrast, negative charge accelerating ESI-MS measurement of **2a** in THF–CH_3CN in the presence of LiCl provided charged peaks of moderate intensity at m/z 548.4 (intensity, 62%), 377.2 (62%), and 206.0 (100%), corresponding to the $[3M + Cl]^-$, $[2M + Cl]^-$, and $[M + Cl]^-$ charge states, respectively, as shown in Fig. 1. Any peaks related to higher oligomers such as tetramers which are likely too strained to form could not be observed at all, affording a further evidence that the trimer arrangement is the most favorite one. Similarly, the ESI-MS measurement of **2b** in THF–CH_3CN in the presence of LiCl afforded charged peaks at 638.5 (11%), 437.5 (54%), and 236.2 (73%), respectively, corresponding to the $[3M + Cl]^-$, $[2M + Cl]^-$, and $[M + Cl]^-$ charge states (Fig. S5 in the ESI†).

In the ^1H and ^{13}C NMR spectra of **2a** and **2b**, only one set of signals as a monomer was observed (Fig. S1–4 in the ESI†). The NOESY spectra of **2a** in $CDCl_3$ showed NOE interactions between the H-2, -6 of the pyridine moiety and protons of the ethyl groups, and the ^{11}B NMR spectra of **2a** displayed a strong signal at −1.52 ppm, as shown in Fig. 2 and 3, respectively,

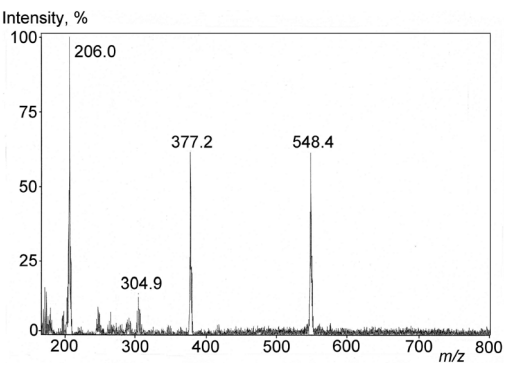

Fig. 1 ESI-MS spectrum of **2a** in the presence of LiCl in THF–CH_3CN.

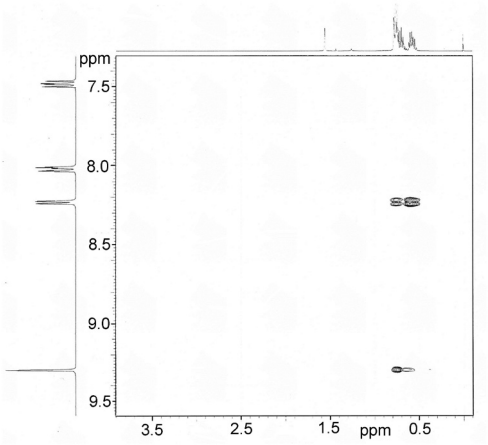

Fig. 2 NOESY spectrum of **2a** (400 MHz, $CDCl_3$).

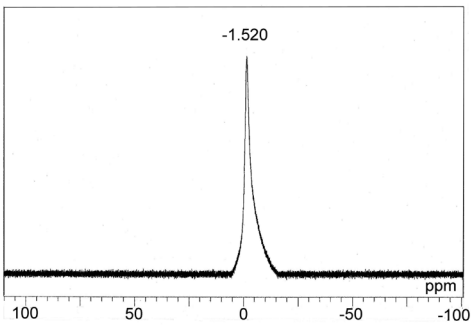

Fig. 3 ^{11}B NMR spectrum of **2a** (192 MHz, $CDCl_3$).

showing that the monomer–oligomer equilibrium is exclusively to the side of the oligomer.[7] Similar observations were obtained from the NOESY and ^{11}B NMR spectra of **2b** (Fig. S6 and S7 in the ESI†). These data clearly indicate that **2** mainly forms a cyclic trimeric assembly *via* intermolecular boron–nitrogen coordination bonds in solution.

Structure in the crystalline state

Compounds **2a** and **2b** could be recrystallized from a mixed solution of 2-propanol and diethylether to give single crystals. However, the crystal structure of **2a** could not be determined by X-ray crystallography, despite obtaining enough reflections from the single crystals. In contrast, the X-ray crystal structure of **2b** was determined easily, and it revealed the formation of a cyclic trimeric structure as shown in Fig. 4. The crystal data and crystallographic refinement parameters of **2b** are summarized in Table 1, and selected bond distances and bond angles are listed in Table 2.

The distance between the boron atom and the nitrogen atom is 1.648 Å, which is slightly longer than that of the tetramer of **1a** (1.638 Å).[2d,e] The bond angles constituted by the boron atom and the three substituents enable calculation of the tetrahedral character (THC) of the boron atom, as proposed by Toyota and Ōki.[8] The THC value for **2b** is estimated to be 80%, which is slightly lower than that of **1a** (82%).[2d,e]

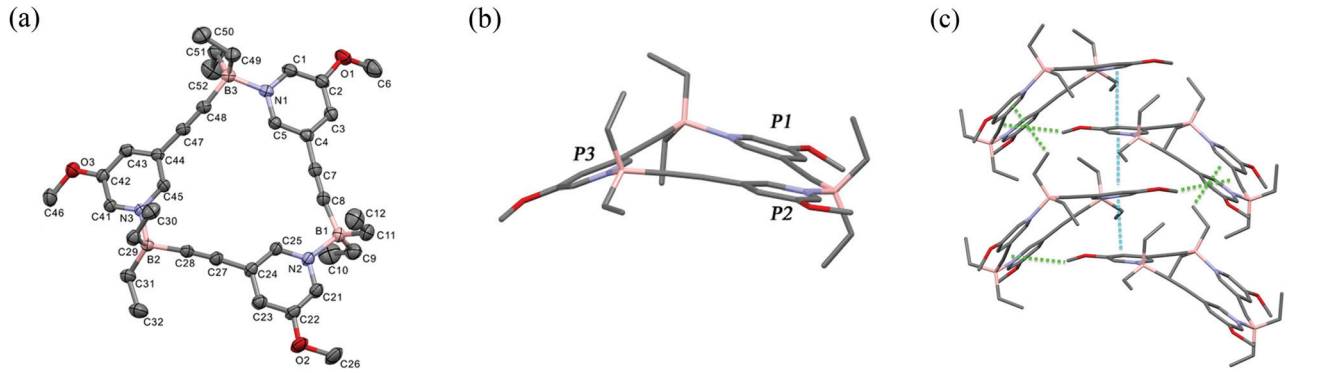

Fig. 4 Crystal structures of the trimer of **2b**. Boron = pink, carbon = gray, nitrogen = blue-gray, oxygen = red. (a) ORTEP drawing with 30% probability displacement ellipsoids. H atoms are omitted for clarity. (b) Stick style. Two pyridine rings (*P*1 and *P*2) are almost coplanar, while the other pyridine ring (*P*3) is largely bent away from *P*1 and *P*2. (c) Packing diagram. The π–π stacking and CH–π interactions are indicated by dashed lines in cyan and light green, respectively.

Table 1 Crystal data and refinement parameters for the cyclic trimer of **2b**[a]

Chemical formula	$C_{36}H_{48}B_3N_3O_3$
Formula mass	603.20
Crystal system	Monoclinic
a/Å	18.3878(11)
b/Å	7.5278(5)
c/Å	26.7776(15)
α/°	90.00
β/°	100.221(2)
γ/°	90.00
Unit cell volume/Å^3	3647.7(4)
Temperature/K	293(2)
Space group	$P2_1/n$
No. of formula units per unit cell, *Z*	4
Radiation type	MoKα
Absorption coefficient, *μ*/mm^{-1}	0.068
No. of reflections measured	25 642
No. of independent reflections	6196
R_{int}	0.0614
Final R_1 values ($I > 2\sigma(I)$)	0.0553
Final w$R(F^2)$ values ($I > 2\sigma(I)$)	0.1425
Final R_1 values (all data)	0.1137
Final w$R(F^2)$ values (all data)	0.1785

[a] Numerals in parentheses are estimated standard deviations.

Table 2 Selected geometric properties of the cyclic trimer of **2b**[a]

Bond distances (Å)			
B(1)–N(2)	1.648(4)	B(2)–C(28)	1.592(4)
B(2)–N(3)	1.648(3)	B(2)–C(29)	1.615(4)
B(3)–N(1)	1.648(4)	B(2)–C(31)	1.629(4)
B(1)–C(8)	1.585(4)	B(3)–C(48)	1.593(4)
B(1)–C(9)	1.605(5)	B(3)–C(49)	1.636(4)
B(1)–C(11)	1.625(4)	B(3)–C(51)	1.603(4)
Bond angles (°)			
N(2)–B(1)–C(8)	107.4(2)	C(28)–B(2)–C(29)	112.7(2)
N(2)–B(1)–C(9)	107.6(2)	C(28)–B(2)–C(31)	109.7(2)
N(2)–B(1)–C(11)	107.1(2)	C(29)–B(2)–C(31)	112.5(2)
C(8)–B(1)–C(9)	111.6(2)	N(1)–B(3)–C(48)	106.3(2)
C(8)–B(1)–C(11)	109.5(2)	N(1)–B(3)–C(49)	104.8(2)
C(9)–B(1)–C(11)	113.3(2)	N(1)–B(3)–C(51)	110.1(2)
N(3)–B(2)–C(28)	106.3(2)	C(48)–B(3)–C(49)	112.1(2)
N(3)–B(2)–C(29)	106.1(2)	C(48)–B(3)–C(51)	109.0(2)
N(3)–B(2)–C(31)	109.3(2)	C(49)–B(3)–C(51)	114.2(2)

[a] Numerals in parentheses are estimated standard deviations.

Therefore, the coordination bonds of the cyclic trimer of **2b** appear to be slightly weaker than those of **1a**.

With regard to the crystal structure, there are several aspects worth commenting. The two pyridine rings (*P*1 and *P*2) of the cyclic trimer of **2b** are almost coplanar (dihedral angle: 5.7°), and the other pyridine ring (*P*3) is bent away from *P*1 and *P*2 by 37.7° and 32.0°, respectively. In addition, one of the pyridine rings (*P*3) of the cyclic trimer of **2b** is aligned face-to-face with one of the pyridine rings (*P*3′) of the adjacent symmetry-related trimer molecule ($5/2 - x$, $-1/2 + y$, $3/2 - z$). The distance between the centers of mass of *P*3 and *P*3′ is 3.942 Å, which corresponds to the typical π–π interaction distance. In contrast, the other two pyridine rings do not overlap with their top and bottom neighbors. For the cyclic trimer of **2b**, theoretical calculations using B3LYP/6-31G* indicate that a completely coplanar assembly is the most stable conformation.[9] The molecular conformation found in the crystal is, however, not coplanar, and the bent conformation is suggested as a relatively stable alternative in the theoretical calculations performed. Therefore, the bent structure of the cyclic trimer of **2b** appears to be necessary for crystallization, and the π–π stacking interaction between *P*3 and *P*3′ plays a dominant role in the packing of the trimer along the *b* axis, which is also maintained by CH–π interactions between $-OCH_3$ of *P*3 and the acetylene moiety adjoining *P*1′ and *P*2′ ($5/2 - x$, $-1/2 + y$, $3/2 - z$), and between $-B(CH_2CH_3)_2$ of *P*3 and *P*2″ (x, $-1 + y$, z). It should be stressed that the packing diagram affects the conformation of the cyclic trimer of **2b**, which may be a flexible molecule in nature.

Scrambling behavior

To gain insight into the effect of the acetylene substituent on the stability of the cyclic trimer, scrambling experiments were conducted using **2a** and **2b**. When an equimolar mixture of **2a**

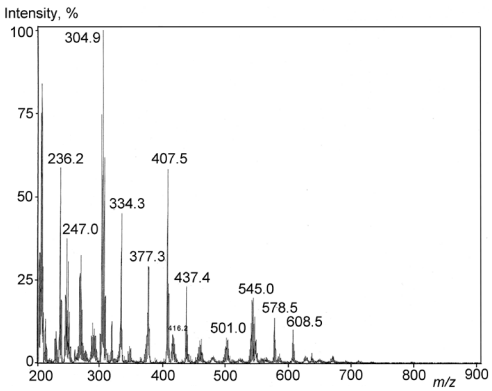

Fig. 5 ESI-MS spectrum of the scrambled products of **2a** and **2b** in the presence of LiCl in THF–CH_3CN.

and **2b** in toluene-d_8 was allowed to stand at room temperature for 3 days, the ^{1}H NMR spectrum remained unchanged. However, upon heating at 80 °C for 6 h, **2a** and **2b** were readily scrambled into trimers. Although the products were not isolated, the scrambled products would give rise to new ^{1}H NMR signals. The ESI-MS spectrum of the scrambled products in THF–CH_3CN in the presence of LiCl showed charged peaks at *m*/*z* 608.5 and 578.5, corresponding to $[(\mathbf{2a})(\mathbf{2b})_2 + Cl]^-$ and $[(\mathbf{2a})_2(\mathbf{2b}) + Cl]^-$, respectively (Fig. 5), which support the formation of scrambled products. Thus, the conditions that led to scrambling (80 °C, 6 h) were milder than the scrambling conditions of **1a** (100 °C, 24 h): this was unexpected since little steric hindrance in **2** would strengthen the B–N coordination bonds compared with **1**. Since scrambling of constituent molecules appears to occur predominantly *via* an S_N1-type mechanism,[2k] the coordination bonds in the trimer of **2** must be weaker than those in the tetramer of **1**.

Furthermore, since the natural-population analysis based on B3LYP/6-31G* calculations on monomer **2a** produced a lower positive charge for the boron atom of **2a** (0.827) compared to that of **1a** (0.928),[9] it appears that the acetylene moiety in **2** reduces the Lewis acidity of the boron atom, thus weakening the intermolecular boron–nitrogen coordination bonds, which is reflected in the molecular structure of the complex as stated above.

Conclusions

A facile method for the synthesis of **2** has been developed. Compound **2** assembles into a cyclic trimer stabilized *via* intermolecular boron–nitrogen coordination bonds. The solution structure of **2** was verified by the NOEs between H-2, -6 of the pyridine moiety and the protons of the ethyl groups, ^{11}B NMR chemical shifts, and VPO data. The structural features of **2b** in the crystalline state unexpectedly include the two pyridine rings (*P*1 and *P*2) with an almost coplanar arrangement and the third pyridine ring (*P*3) that is bent away from *P*1 and *P*2, affording a partially face-to-face stacked assembly, which is maintained by π–π stacking and CH–π interactions. The crystallographic study revealed that the conformation of the cyclic trimer is flexible enough to be affected by the crystal packing. The present study provides some important information on the mechanism of self-assembly, and, therefore, may be helpful in the construction of novel self-assembled molecular systems.

Experimental

3-(Diethylborylethynyl)pyridine (2a)

To a solution of 3-ethynylpyridine (322 mg, 3.1 mmol) in ether (10 mL) was added a 1.5 M hexane solution of *n*-butyllithium (2.3 mL, 3.5 mmol) at −78 °C. After stirring at the same temperature for 1 h, a 1 M THF solution of diethylmethoxyborane (7.8 mL, 7.8 mmol) was added. The temperature of the mixture was gradually raised to 0 °C over 1 h and stirred for 0.5 h. The reaction mixture was poured into water (20 mL) and extracted with ether (80 mL, 20 mL). The organic layer was washed with brine, dried over $MgSO_4$, and concentrated. The crude product was subjected to column chromatography using silica gel (7 g) and benzene–hexane (1 : 2) as the eluent to afford **2a** (381 mg, 72%) as a colorless solid. mp. >180 °C (dec). ^{1}H NMR (400 MHz, $CDCl_3$): 0.52–0.78 (m, 10H), 7.48 (dd, 1H, *J* = 5.9, 7.8 Hz), 8.02 (dt, 1H, *J* = 1.7, 7.8 Hz), 8.23 (d, 1H, *J* = 5.9 Hz), 9.30 (d, 1H, *J* = 1.7 Hz). ^{13}C NMR (100 MHz, $CDCl_3$): 10.4, 17.9, 93.5, 124.7, 125.5, 140.5, 142.2, 148.0. ^{11}B NMR (192 MHz, $CDCl_3$): −1.52. IR (KBr): 2939, 2862, 2172, 1479, 1416, 1250, 1101, 1045 cm^{-1}. UV/vis ($CHCl_3$): 261 (ε 14 900), 302 (6430) nm. EIMS (20 eV): *m*/*z* 171 (M^+, 61%), 142 (M^+ − Et, 100). HRMS (EI): *m*/*z* calcd for $C_{11}H_{14}BN$ 171.12193, found 171.12156. Anal. Calcd for $C_{11}H_{14}BN$: C, 77.24; H, 8.25; N, 8.19. Found. C, 77.15; H, 8.58; N, 8.27.

3-(Diethylborylethynyl)-5-methoxypyridine (2b)

To a solution of 3-ethynyl-5-methoxypyridine (200 mg, 1.49 mmol) in ether (7 mL) was added a 1.5 M hexane solution of *n*-butyllithium (1.1 mL, 1.65 mmol) at −70 °C. After stirring at the same temperature for 1 h, diethylmethoxyborane (0.5 mL, 3.8 mmol) was added. The temperature of the mixture was gradually raised to 0 °C over 1 h and stirred for 0.5 h. The reaction mixture was poured into water (20 mL) and extracted with ether (40 mL, 10 mL). The organic layer was washed with brine, dried over $MgSO_4$, and concentrated. The crude product was subjected to column chromatography using silica gel (4 g) and benzene–hexane (1 : 1) as the eluent to afford **2b** (238 mg, 79%) as a colorless solid. mp. >150 °C (dec). ^{1}H NMR (400 MHz, $CDCl_3$): 0.55–0.76 (m, 10H), 3.93 (s, 3H), 7.50 (dd, 1H, *J* = 1.4, 2.5 Hz), 7.91 (d, 1H, *J* = 2.7 Hz), 8.90 (d, 1H, *J* = 1.2 Hz). ^{13}C NMR (100 MHz, $CDCl_3$): 10.4, 18.0, 56.2, 93.6, 125.6, 128.3, 130.1, 140.6, 156.6. ^{11}B NMR (192 MHz, $CDCl_3$): −1.60. IR (KBr): 2940, 2862, 2172, 1583, 1449, 1418, 1321, 1198 cm^{-1}. UV/vis ($CHCl_3$): 240 (ε 16 900), 265 (9040), 312 (8990) nm. EIMS (20 eV): *m*/*z* 201 (M^+, 93%), 172 (M^+ − Et, 100). HRMS (EI): *m*/*z* calcd for $C_{12}H_{16}BNO$ 201.13249, found 201.13273. Anal. Calcd for $C_{12}H_{16}BNO$: C, 71.68; H, 8.02; N, 6.97. Found. C, 71.69; H, 8.21; N, 7.00.

Vapor pressure osmometry results for 2a and 2b

2a: average aggregate size: 3.1 in acetone at 40 °C [benzil (88.5, 271.3, 494.8, 1008 for 0.005, 0.019, 0.037, 0.070 mol dm^{-3}, respectively), **2a** (63.5, 147, 235, 388 for 0.012, 0.030, 0.050, 0.083 mol dm^{-3}, respectively)]; 2.8 in chloroform at 45 °C [benzil (76.5, 274, 596, 1067 for 0.006, 0.020, 0.044, 0.077 mol dm^{-3}, respectively), **2a** (75.3, 185, 273, 410 for 0.012, 0.030, 0.050, 0.083 mol dm^{-3}, respectively)]; 2.8 in benzene at 60 °C [benzil (83, 278, 561, 1019 for 0.006, 0.021, 0.041, 0.075 mol dm^{-3}, respectively), **2a** (55.5, 139.3, 227, 378 for 0.011, 0.028, 0.046, 0.077 mol dm^{-3}, respectively)]; **2b**: average aggregate size: 3.3 in chloroform at 40 °C [benzil (9.5, 33.3, 58.4, 87.3 for 0.006, 0.020, 0.035, 0.051 mol dm^{-3}, respectively), **2b** (10.0, 17.0, 31.0, 45.9 for 0.019, 0.031, 0.052, 0.087 mol dm^{-3}, respectively)]; 2.9 in THF at 45 °C [benzil (11.0, 33.1, 59.7, 85.9 for 0.006, 0.020, 0.035, 0.051 mol dm^{-3}, respectively), **2b** (11.6, 18.5, 29.7, 51.1 for 0.019, 0.031, 0.052, 0.087 mol dm^{-3}, respectively)], 3.2 in benzene at 60 °C [benzil (10.4, 34.8, 60.9, 88.1 for 0.006, 0.020, 0.035, 0.051 mol dm^{-3}, respectively), **2b** (8.5, 15.3, 27.4, 46.3 for 0.019, 0.032, 0.053, 0.088 mol dm^{-3}, respectively)], aggregate size: 1.5–2.7 in *N*,*N*-dimethylformamide at 90 °C [benzil (4.8, 17.2, 29.8, 42.0 for 0.006, 0.020, 0.035, 0.051 mol dm^{-3}, respectively), **2b** (5.5, 13.3, 27.9, 37.3 for 0.017, 0.029, 0.048, 0.081 mol dm^{-3}, respectively)].

Crystallographic study

Compound **2b** was saturated in a mixed solution of 2-propanol and diethyl ether (1 : 1), which was slowly evaporated at 293 K to obtain single crystals. X-ray diffraction data were collected on a Rigaku RAXIS-RAPIDII imaging plate area detector using graphite-monochromated Mo-K radiation (λ = 0.710690 Å) at 293 K. Frame data were integrated, and the dataset was corrected for absorption using a Rigaku/MSC CrystalClear program package. All calculations were performed with a Rigaku/MSC CrystalStructure program package and structures were solved by Direct Methods (SIR92)[10] and refined on F^2 by full-matrix least squares techniques (SHELXL 97).[11] Anisotropic refinement was applied to all nonhydrogen atoms. All hydrogen atoms were placed at calculated positions. The structural drawing and geometrical calculations were performed with the MERCURY[12] and PLATON[13] software. Further details of the crystal structure determination are given in Table 1, and the selected intramolecular bond distances and angles are listed in Table 2.

Theoretical calculations

All theoretical calculations were performed using the *Spartan '10* computer modeling software.[9] The geometry of the cyclic trimer of **2b** was optimized by the conformation search with molecular mechanics calculations using the MMFF force field, followed by DFT calculations at the B3LYP/6-31G* level.

Acknowledgements

S. W. gratefully acknowledges financial support from The Nishida Research Fund for Fundamental Organic Chemistry and Mie Prefecture. We are also grateful to Prof. M. Shimizu of Mie University for the valuable discussions, Profs Y. Tobe and K. Hirose of Osaka University for their help with VPO, and Dr K.-I. Oyama and Mr Y. Maeda of Nagoya University for their help with MS and NMR spectroscopy.

Notes and references

1 (*a*) M. L. Cragg, *Organoboranes in Organic Synthesis*, M. Dekker, New York, 1973; (*b*) H. C. Brown, *Organic Synthesis via Boranes*, John Wiley & Sons, Inc., New York, 1975; (*c*) E. Negishi, *J. Organomet. Chem.*, 1976, **108**, 281; (*d*) N. Miyaura and A. Suzuki, *Chem. Rev.*, 1995, **55**, 2457.

2 (*a*) E. Hanecker, T. G. Hodgkins, K. Niedenzu and H. Nöth, *Inorg. Chem.*, 1985, **24**, 459; (*b*) C. P. Brock, A. L. Companion, L. D. Kock and K. Niedenzu, *Inorg. Chem.*, 1991, **30**, 784; (*c*) T. G. Hodgkins, *Inorg. Chem.*, 1993, **32**, 6115; (*d*) Y. Sugihara, R. Miyatake, K. Takakura and S. Yano, *J. Chem. Soc., Chem. Commun.*, 1994, 1925; (*e*) Y. Sugihara, K. Takakura, T. Murafuji, R. Miyatake, K. Nakasuji, M. Kato and S. Yano, *J. Org. Chem.*, 1996, **61**, 6829; (*f*) T. G. Hodgkins and D. R. Powell, *Inorg. Chem.*, 1996, **35**, 2140; (*g*) T. Murafuji, R. Mouri, Y. Sugihara, K. Takakura, Y. Mikata and S. Yano, *Tetrahedron*, 1996, **52**, 13933; (*h*) S. Wakabayashi, Y. Sugihara, K. Takakura, S. Murata, H. Tomioka, S. Ohnishi and K. Tatsumi, *J. Org. Chem.*, 1999, **64**, 6999; (*i*) V. Barba, H. Höpfl, N. Farfán, R. Santillan, H. I. Beltran and L. S. Zamudio-Rivera, *Chem. Commun.*, 2004, 2834; (*j*) V. Barba, R. Villamil, R. Luna, C. Godoy-Alcántar, H. Höpfl, H. I. Beltran, L. S. Zamudio-Rivera, R. Santillan and N. Farfán, *Inorg. Chem.*, 2006, **45**, 2553; (*k*) S. Wakabayashi, S. Imamura, Y. Sugihara, M. Shimizu, T. Kitagawa, Y. Ohki and K. Tatsumi, *J. Org. Chem.*, 2008, **73**, 81; (*l*) N. Christinat, R. Scopelliti and K. Severin, *Chem. Commun.*, 2008, 3660.

3 (*a*) S. Sato, Y. Ishido and M. Fujita, *J. Am. Chem. Soc.*, 2009, **131**, 6064; (*b*) Q.-F. Sun, J. Iwasa, D. Ogawa, Y. Ishido, S. Sato, T. Ozeki, Y. Sei, K. Yamaguchi and M. Fujita, *Science*, 2010, **328**, 1144; (*c*) N. Ponnuswamy, G. D. Pantoş, M. M. J. Smulders and J. K. M. Sanders, *J. Am. Chem. Soc.*, 2012, **134**, 566; (*d*) K. Tambara, J.-C. Olsen, D. E. Hansen and G. D. Pantoş, *Org. Biomol. Chem.*, 2014, **12**, 607.

4 The cavity size of the cyclic tetramer of **1a** and 3-dimethylborylpyridine is estimated to be *ca.* 1.5–1.7 Å[2d,e] and 1.3–1.7 Å,[2k] respectively.

5 3-Ethynylpyridine was prepared in two steps: (1) coupling reaction of 3-bromopyridine with 2-methyl-3-butyn-2-ol in the presence of $PdCl_2(PPh_3)_2$ and CuI in DMF–triethylamine at 95 °C for 1 h, and (2) treatment with KOH in benzene at 90 °C for 1 h in 51% overall yield.

6 3-Ethynyl-5-methoxypyridine was prepared by the similar method to 3-ethynylpyridine, starting from 3-bromo-5-methoxypyridine in 61% yield.

7 The boron of **2a** and **2b** are found to resonate at a far higher position than that of the trivalent boron, for example,

1-(dimesitylboryl)-4-(dimethylamino)benzene (71.5 ppm). The marked shielding of the boron in the trimethylborane-trimethylamine adduct (−0.1 ppm) and the trimethylborane-pyridine adduct (0.0 ppm) is ascribed to the coordination bond between the trivalent boron and the nitrogen of amines. See: (*a*) H. Nöth and H. Vahrenkamp, *Chem. Ber.*, 1966, **99**, 1049; (*b*) H. Nöth and B. Wrackmeyer, *Chem. Ber.*, 1974, **107**, 3070, and ref. 2*d*,*e*,*g*,*h*,*k*.

8 S. Toyota and M. Ōki, *Bull. Chem. Soc. Jpn.*, 1992, **65**, 1832.

9 *Spartan '10*, Wavefunction, Inc., Irvin, CA, 2010.

10 A. Altomare, G. Cascarano, C. Giacovazzo and A. Guagliardi, *J. Appl. Crystallogr.*, 1993, **26**, 343.

11 G. M. Sheldrick, University of Göttingen, Germany, 1997.

12 C. F. Macrae, I. J. Bruno, J. A. Chisholm, P. R. Edgington, P. McCabe, E. Pidcock, L. Rodriguez-Monge, R. Taylor, J. van de Streek and P. A. Wood, *J. Appl. Crystallogr.*, 2008, **41**, 466.

13 A. L. Spek, *Acta Crystallogr., Sect. D: Biol. Crystallogr.*, 2009, **65**, 148.